

# Band Gap and Density of States of the Hydrated C<sub>60</sub> Fullerene System at Finite Temperature

Roberto Rivelino\* and F. de Brito Mota\*

*Instituto de Física, Universidade Federal da Bahia, 40210-340 Salvador, Bahia, Brazil*

*Received February 7, 2007; Revised Manuscript Received May 3, 2007*

## ABSTRACT

We examine the electronic properties of the hydrated C<sub>60</sub> fullerene under ambient conditions using a sequential Monte Carlo/density functional theory scheme. In this procedure, the average electronic properties of the first hydration shell of C<sub>60</sub> equilibrate for ca. 40 uncorrelated configurations of the fullerene aqueous solution. We obtain a systematic red-shift of 0.8 eV in the band gap of the hydrated system, which is mainly attributed to the thermal fluctuations of the aqueous environment.

Advances in molecular-scale technology have emerged rapidly from the possibility to deal with nanostructures using first-principles theoretical methodologies. As expected by the electronics industry, molecular sensing devices based on semiconductor nanoparticles<sup>1</sup> have attracted a great interest for application in biological systems, mostly because of the efficiency of their optical properties.<sup>2</sup> In practice, the study of these materials as biosensors requires including the aqueous environment in order to evaluate the absorption and emission of light. Thus it is worthwhile to have a careful and complete understanding of the interactions between a nanostructure and the surrounding water molecules in using as optical tags. In this case, the strength of these interactions, together with the spatial confinement effects of the medium, may drastically change the properties of the system.

Among several nanometer-size materials with potential biological importance, fullerenes have been pointed out to be one of the most versatile structures. For example, dispersions of pure C<sub>60</sub> in water seem to play a crucial role for therapeutic purpose<sup>3,4</sup> and cytotoxicity<sup>5</sup> as well. In addition, fullerene (C<sub>60</sub>) spheres have been investigated as possible Raman active nanosensors<sup>6</sup> and still employed to increase the biostability of electrochemical sensors<sup>7</sup> based on bilayer lipid membrane. From these and other motivations, obtaining stable water-soluble forms of pristine fullerenes has become one of the greatest challenges of nanoscience nowadays.<sup>8–10</sup> Despite the very low solubility of fullerenes in aqueous medium,<sup>11</sup> stable solutions with different concentrations have been prepared<sup>12–14</sup> and studied by using different techniques.<sup>13–18</sup> Even though there exist many experimental data available to assess the structure of hydrated

fullerenes, the interaction between these carbon compounds with water is not yet well understood, and much of this understanding lies in hydrophobic driving forces which influence the solute aggregation on larger length scales.<sup>19,20</sup> Indeed, a conceptual basis capable to describe the water–carbon interaction in fullerenes should involve an effective intermolecular potential model that accounts for the dispersion interaction.<sup>21</sup> It has been demonstrated, via molecular dynamics simulation, that the C<sub>60</sub>–water interaction is dominated by relatively strong van der Waals attraction.<sup>22</sup> Doubtless, an accurate description at this level is also of special interest for comprehension of the properties of closely related systems such as wetting graphite surfaces<sup>23</sup> and water-filled carbon nanotubes.<sup>24</sup>

Recently, we have investigated the water hydrogen-bonding features near the surface of C<sub>60</sub> and the UV–vis absorption properties of the hydrated fullerene, obtained from Monte Carlo (MC) simulation for a dilute aqueous solution in ordinary thermodynamic conditions (ref 25). Our calculated average optical absorption spectra of the hydrated system after performing the MC simulation, including dispersion interactions between the two subsystems,<sup>26</sup> fairly showed a very good agreement with experimental data.<sup>13,18</sup> Also, our statistical analysis has reinforced the supposed existence of supramolecular hydrated clusters C<sub>60</sub>@{H<sub>2</sub>O}<sub>m</sub> in aqueous environments, which has more recently been proposed to be in connection with DNA damage in human lymphocytes.<sup>12</sup> In this letter, we explore the possibility of understanding a fullerene aqueous solution by surveying the dielectric screening of water on the band gap and density of states (DOS) of the hydrated solute at room temperature and atmospheric pressure. Following this purpose, we can evaluate the hydration effects on the system C<sub>60</sub> because the

\* Corresponding authors. E-mail: rivelino@ufba.br (R.R.); fbmota@ufba.br (F.B.M.). Fax: +55-71-3263-6606.

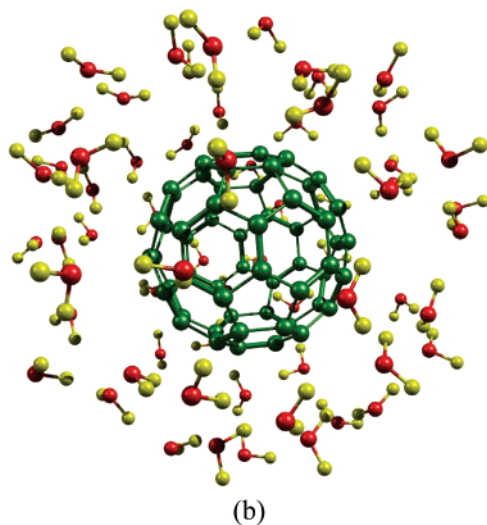
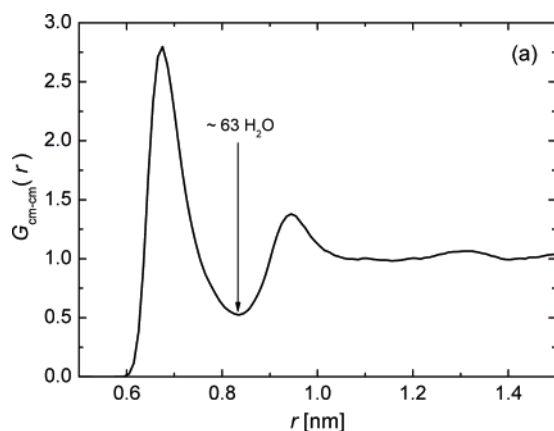


**Figure 1.** (a) Pairwise RDF between the centers of mass of  $C_{60}$  and water. First peak shows the hydration shell containing ca. 63 water molecules, obtained by spherical integration of  $G_{\text{cm-cm}}(r)$  from the solute center-of-mass up to the limit of the first shell. (b) One out of the uncorrelated MC configurations constituents of the first hydration shell of  $C_{60}$ .

strength of the solute–solvent interaction determines how much the band gap of the hydrated fullerene deviate from that of its isolated form.

The scheme to treat these effects is based on a systematic approach combining MC simulation with quantum mechanical calculations (QM), i.e., the sequential MC/QM procedure.<sup>27–31</sup> First, a standard MC simulation<sup>32</sup> is performed over one  $C_{60}$  molecule solvated by 1000 water molecules at 298 K and 1 atm using the *NPT* ensemble to generate the configurations of the fullerene aqueous solution. A 60-site Lennard-Jones (LJ) potential model<sup>22,23,25</sup> has been employed to consider the dispersion interaction between fullerene and water, and the five-site TIP5P potential model,<sup>33</sup> which reproduces high-quality structural and thermodynamic properties of water, is employed here to describe the intermolecular interactions of the aqueous medium. Our simulation is carried out in a periodic cubic cell using the DICE code.<sup>34</sup> The long-range water–water Coulomb interactions have been treated with the reaction field method, while LJ interactions have been truncated at the cutoff radius of 1.6 nm. After equilibration of  $10^7$  MC steps, the sampling is performed

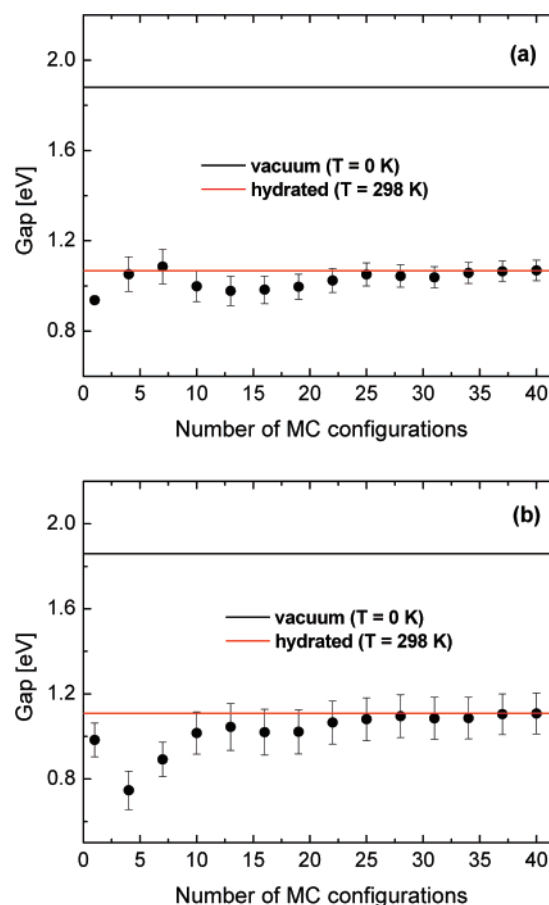


**Figure 2.** Band gap convergence of the hydrated system ( $C_{60}$  surrounded by 63 water molecules in each MC configuration) at room temperature. The values are computed at the (a) LDA and (b) BLYP levels of DFT, using eq 1. The average values are shown (red line) and also the corresponding gap of the isolated  $C_{60}$  (black line).

over a running length of  $1.0 \times 10^8$  additional MC steps. Second, for the QM calculations, we use first-principles density functional theory (DFT) methods to obtain the properties of only statistically relevant configurations of the hydrated system, which have been separated via procedures described elsewhere.<sup>25,27–31,35</sup> This methodology reduces significantly thousands of MC configurations of the aqueous solution to hundreds of uncorrelated configurations.

At the DFT level, the calculations are carried out using the SIESTA program<sup>36</sup> to solve the Kohn–Sham (KS) self-consistent equations. These are done within two common approaches: (i) the local density approximation (LDA) with the exchange–correlation term taken from Ceperley–Alder data,<sup>37</sup> as parametrized by Perdew–Zunger,<sup>38</sup> and (ii) the gradient-corrected approximation (GGA) with the BLYP proposal.<sup>39</sup> A nonlocal norm-conserving scalar Troullier–Martins<sup>40</sup> pseudopotential has been included to replace the core electrons, and the KS eigenstates are expanded using a linear combination of numerical atomic orbitals (NAO) as the basis set. In the LDA approach, we utilize a split-valence double- $\zeta$  basis set with polarization function (DZP), specially optimized for water and fullerene,<sup>41</sup> whereas in the GGA approach, we employ the usual scheme<sup>42</sup> of obtaining DZP NAO basis sets. In this case, an equivalent plane-wave cutoff

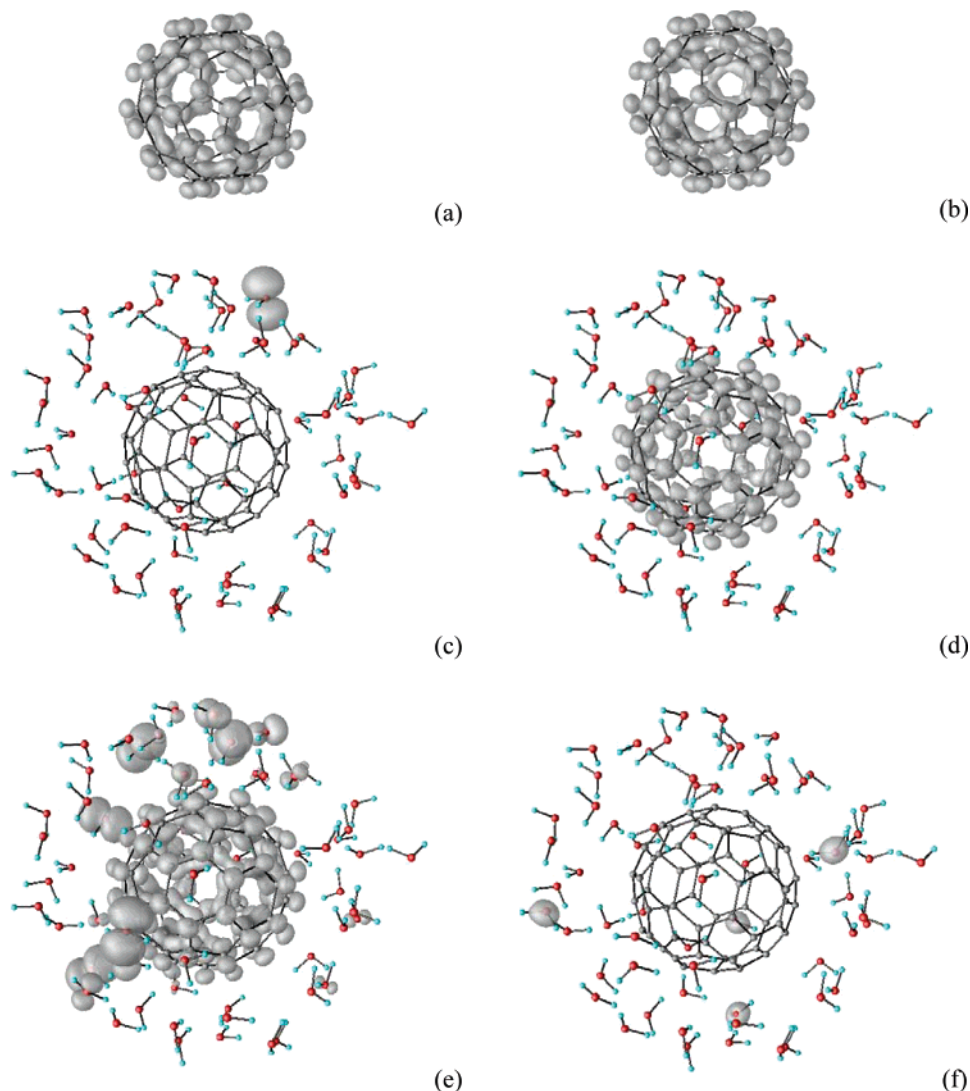


**Figure 3.** Electron densities of the Kohn–Sham eigenstates near the Fermi level: (a) HOMO and (b) LUMO of the isolated fullerene, (c) lone pairs of water, (d) LUMO, (e) top of the valence band, and (f) innermost orbital at  $-23.5$  eV of a specific configuration constituent of the first hydration shell of  $C_{60}$ .

radius of 200 Ry for the grid integration is utilized to represent the charge density. Only the  $\Gamma$   $k$ -point in the Brillouin zone has been used in these calculations. Finally, the electronic properties of the hydrated system are obtained as averages over uncorrelated supramolecular structures, composed of one  $C_{60}$  molecule surrounded by its first solvation shell, explicitly included in the DFT calculations.

As calculated from the simulated center-of-mass radial distribution function (RDF),  $G_{\text{cm-cm}}(r)$  given in Figure 1a, 63 water molecules on average are present in each configuration representing the first solvation shell of fullerene, i.e., our system of interest corresponds to structurally different clusters of the  $C_{60}@[\text{H}_2\text{O}]_{63}$  type (Figure 1b). This result is rather similar to that obtained in our previous investigation<sup>25</sup> using the SPC potential for describing the aqueous medium, although the hydrating water molecules form a more well-ordered shell around  $C_{60}$  with the TIP5P model. In Figure 2, we show the band gap ( $E_g$ ) convergence of the hydrated fullerene as a function of the number of uncorrelated MC configurations included in the averaging. Our calculated  $E_g$

(eq 1) is a mean difference between the KS eigenvalues of the highest occupied molecular orbital (HOMO) and lowest unoccupied molecular orbital (LUMO) of the ground-state electronic structure of the hydrated system over only uncorrelated configurations, as given by

$$\langle E_g \rangle = \left( \frac{1}{L} \right) \sum_{i=1}^L E_g(i) \quad (1)$$

The results for a Markov chain of size  $L = 40$  are completely converged at both level of calculations LDA and GGA (Figure 2). This procedure, involving average electronic properties of uncorrelated supramolecular structures  $C_{60}@[\text{H}_2\text{O}]_{63}$ , is our picture of the liquid-state system.

By using the MC/DFT method, the average band gap of the hydrated system is calculated as  $1.07 \pm 0.28$  eV with LDA and  $1.11 \pm 0.31$  eV with GGA. The two levels of DFT also give good estimates for the HOMO–LUMO gap of  $C_{60}$  in vacuum, i.e., 1.88 and 1.86 eV, respectively. For com-

parison, this energy gap determined for  $C_{60}$  aggregates from direct forbidden optical transitions<sup>16</sup> data is 1.77 eV. The hydrated system displays a systematic red-shift of 0.8 eV from the isolated fullerene at 0 K using LDA or GGA approaches. This coincidence for both DFT levels clearly ensures that we are dealing with converged results. However, this shift is not an effect caused by the polarization of the surrounding solvent on the solute. Instead, the main contribution for this shift is due to structural fluctuations of the hydrating water around  $C_{60}$  at room temperature, as we will examine later for the calculated DOS. A similar result was also observed for the absorption gap of small silicon clusters<sup>1</sup> in the presence of water, with a red-shift of 0.7 eV obtained by first-principles molecular dynamics. In fact, a discussion more related to the polarization effect on fullerenes can be done considering our previous work,<sup>25</sup> using singly excited configuration interaction calculations, for obtaining the optical absorption spectra of the hydrated  $C_{60}$ . In this case, we have estimated a very mild red-shift of  $\sim 0.2$  eV (and  $\sim 0.1$  eV, experimentally<sup>18</sup>) as resulting from the solute–solvent interaction under ambient conditions. Thus, the dielectric screening of water is not expected to produce a significant charge redistribution effect on the fullerene surface.

Figure 3 illustrates the charge densities related to the KS eigenstates near the Fermi level for the isolated  $C_{60}$  and for a random configuration taken from the MC simulation of the aqueous solution at 298 K. In the one-particle framework, the electronic ground state of pristine  $C_{60}$  is constituted by a 5-fold degenerate HOMO (represented in Figure 3a) and a 3-fold degenerate LUMO (represented in Figure 3b), separated by a small energy gap ( $\sim 1.8$  eV). It is quite interesting to notice that the higher occupied states of the solvated system (Figure 3c) are localized in electron lone pairs of oxygen atoms of the hydrating molecules, whereas the lowest unoccupied states of the hydrated fullerene (Figure 3d) are qualitatively similar to the LUMO of the isolated solute. These findings are opposed to those observed in hydrated silicon clusters,<sup>1</sup> for which the HOMO was not affected by solvation and the LUMO coincided with the one of the solvent. This can be explained because the band gap of  $C_{60}$  is rather smaller compared to that of Si clusters and the still larger band gap of liquid water.<sup>43</sup> However, our results are in agreement with the expected high electron affinity of  $C_{60}$  as in the presence of available oxygen and water.<sup>5,13</sup> In other words, this reveals the weak donor–acceptor character of the interactions involving electron lone pairs of oxygen atoms on  $H_2O$  and the fullerene surface. To examine the one-particle states near the Fermi level of the solvated system, we compare its calculated DOS with that of the isolated  $C_{60}$  (Figure 4). Our energy scale is adjusted using the Fermi energy level so that the lowest valence  $s$ -states of the oxygen atoms are aligned at ca.  $-23.5$  eV (illustrated in Figure 3f). For clarity, we do not represent the innermost energy states in the DOS depicted in Figure 4.

As noticed before, the higher occupied KS states of the hydrated  $C_{60}$  consist of lone pairs on water molecules, as seen in Figure 3c and indicated in Figure 4b (w-lp). Then,

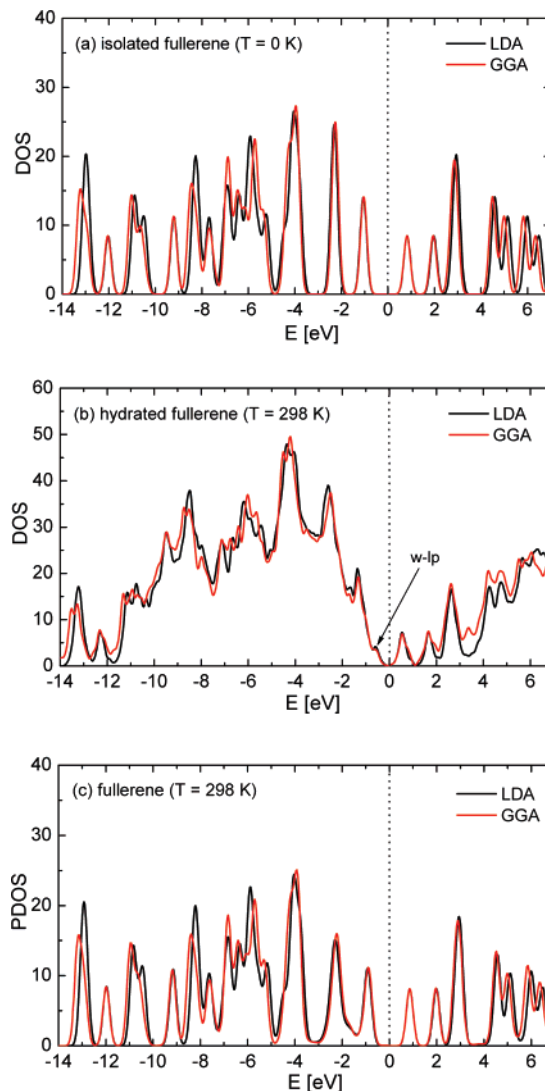


**Figure 4.** (a) Density of states (DOS) of the isolated  $C_{60}$ , (b) the hydrated fullerene, and (c) projected DOS (PDOS) of  $C_{60}$  from the hydrated system. The DOS represented in (b) is an average over 40 uncorrelated MC configurations at ambient conditions.

the higher occupied states of  $C_{60}$ , resembling the HOMO of the isolated fullerene (Figure 4a), are immersed in the valence band of the solvent. Actually, these states represent a mixed contribution of occupied states of  $C_{60}$  and lone pairs of water, which are also illustrated in Figure 3e for a small energy range of  $-1.67$  to  $-0.97$  eV. In this sense, to evaluate the solvent influence on the solute states, we analyze the projected DOS of  $C_{60}$  from the hydrated system (PDOS shown in Figure 4c). Indeed, this clearly reinforces that the influence of the first hydration shell should produce a negligible polarization effect on the fullerene surface. Thus, from the one-particle model analysis of the energy difference between the HOMO and LUMO of  $C_{60}$  in the presence of water, we calculate a small average shift of ca. 0.1 eV as a possible solvent effect on the band gap of the solute.

Otherwise, the KS states of the hydrated fullerene, appearing as a shoulder near the top of the valence band, are originated from thermal fluctuations in the supramolecular structures  $C_{60}@H_2O_{63}$ . To verify this point, in Figure

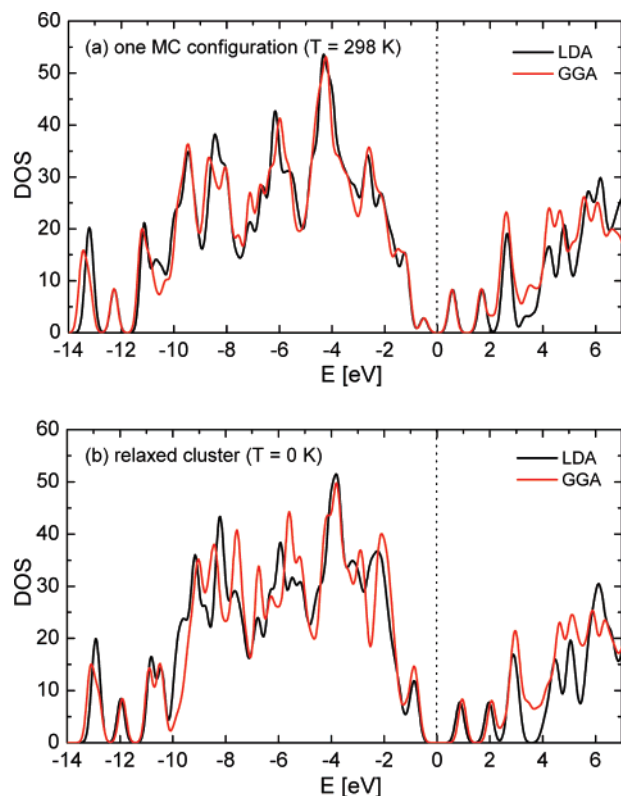


**Figure 5.** (a) DOS of one of the uncorrelated MC configurations of the hydrated  $C_{60}$  and (b) the relaxed  $C_{60}@[H_2O]_{63}$  cluster in vacuum for components of forces smaller than 0.1 eV/Å. It is noticed that the isolated occupied state within the band gap coalesces in the valence band as the temperature is turned off.

5 we compare the DOS obtained for only one out of the uncorrelated MC configurations of the hydrated system ( $T = 298$  K) with the corresponding relaxed hydrated cluster in vacuum ( $T = 0$  K). It is seen that the finite temperature gives rise to an occupied localized state in the band gap (Figure 5a), whereas in the relaxed cluster at 0 K, this state coalesces in the valence band of the more ordered hydrated system (Figure 5b). Finally, taking the room temperature effect into account for the isolated  $C_{60}$ , we expect that no appreciable changes in the electronic structure may be observed due to the rigid surface of this molecule. As a consequence, the calculated 0.8 eV red-shift in the band gap of the hydrated fullerene, from that of the solute in vacuum, indicates that the disordering of water only affects the ground-state electronic structure of the whole system at higher temperature.

In summary, we have used a very efficient sequential MC/DFT scheme<sup>25,27–31,35</sup> to examine the effects of hydration on the band gap and DOS of  $C_{60}$  under ambient conditions. The structures of the hydrated fullerene are properly generated by atomistic MC simulation using a realistic LJ potential.<sup>22,23,25</sup> In this sense, our procedure avoids the lack of dispersion energy inherent to ab initio molecular dynamics simulations based on DFT.<sup>44</sup> The fact also in our favor is that, at finite temperature, dispersion interactions play a much smaller role in the stability of the two subsystems. Then, we obtain reliable average electronic properties of the hydrated system, converging rapid and systematically with

LDA or GGA calculations, which have been proven to successfully work for both liquid water and fullerene.<sup>41–44</sup> As far as we are aware, this is the first theoretical investigation of the finite temperature impact on the electronic structure of the hydrated  $C_{60}$  fullerene using first-principles DFT calculations. Our analysis considers thermal equilibration of an aqueous solution and the dielectric screening of the first solvation shell of  $C_{60}$ . We find that thermal fluctuations of the aqueous environment around the fullerene surface are the most probable sources of the calculated 0.8 eV red-shift in the band gap of the hydrated system. On the other hand, because of the large thermal stability of the electronic structure of  $C_{60}$  in aqueous medium, we do not expect a significant shift in its band gap. This is in agreement with the experimental prediction,<sup>16</sup> from both direct and indirect optical transition data, for  $C_{60}$  aggregates in aqueous environment.

**Acknowledgment.** This work has been partially supported by the Brazilian agencies Fapesb and CNPq.

## References

- (1) Prendergast, D.; Grossman, J. C.; Williamson, A. J.; Fattebert, J.-L.; Galli, G. *J. Am. Chem. Soc.* **2004**, *126*, 13827.
- (2) Eckhoff, D. A.; Sutin, J. D. B.; Clegg, R. M.; Gratton, E.; Rogozhina, E. V.; Braun, P. V. *J. Phys. Chem. B* **2005**, *109*, 19786.
- (3) Gharbi, N.; Pressac, M.; Hadchouel, M.; Szwarc, H.; Wilson, S. R.; Moussa, F. *Nano Lett.* **2005**, *5*, 2578.
- (4) Scharff, P.; Carta-Abelmann, L.; Siegmund, C.; Matyshevska, O. P.; Prylutska, S. V.; Koval, T. V.; Golub, A. A.; Yashchuk, V. M.; Kushnir, K. M.; Prylutsky, Yu. I. *Carbon* **2004**, *42*, 1199.
- (5) Sayes, C. M.; Fortner, J. D.; Guo, W.; Lyon, D.; Boyd, A. M.; Ausman, K. D.; Tao, Y. J.; Sitharaman, B.; Wilson, L. J.; Hughes, J. B.; West, J. L.; Colvin, V. L. *Nano Lett.* **2004**, *4*, 1881.
- (6) Maguire, J. F.; Amer, M. S.; Busbee, J. *Appl. Phys. Lett.* **2003**, *82*, 2592.
- (7) Szymanska, I.; Radecka, H.; Radecki, J.; Kikut-Ligaj, D. *Biosens. Bioelectron.* **2001**, *16*, 911.
- (8) Ko, W.-B.; Heo, J.-Y.; Nam, J.-H.; Lee, K.-B. *Ultrasonics* **2004**, *41*, 727.
- (9) Brant, J. A.; Labille, J.; Bottero, J.-Y.; Wiesner, M. R. *Langmuir* **2006**, *22*, 3878.
- (10) Khokhryakov, A. O.; Avdeev, M. V.; Aksenov, V. L.; Bulavin, L. A. *J. Mol. Liq.* **2006**, *127*, 73.
- (11) Marcus, Y.; Smith, A. L.; Korobov, M. V.; Mirakyan, A. L.; Avramenko, N. V.; Stukalin, E. B. *J. Phys. Chem. B* **2001**, *105*, 2499.
- (12) Dhawan, A.; Taurozzi, J. S.; Pandey, A. K.; Shan, W.; Miller, S. M.; Hashsham, S. A.; Tarabara, V. V. *Environ. Sci. Technol.* **2006**, *40*, 7394.
- (13) Andrievsky, G. V.; Klochkov, V. K.; Bordyuh, A.; Dovbeshko, G. I. *Chem. Phys. Lett.* **2002**, *364*, 8.
- (14) Avdeev, M. V.; Khokhryakov, A. A.; Tropin, T. V.; Andrievsky, G. V.; Klochkov, V. K. *Langmuir* **2004**, *20*, 4363.
- (15) Andrievsky, G. V.; Klochkov, V. K.; Kariakina, E. L.; Mchedlov-Petrosyan, N. O. *Chem. Phys. Lett.* **1999**, *300*, 39.
- (16) Prylutsky, Yu. I.; Durov, S. S.; Bulavin, L. A.; Adamenko, I. I.; Moroz, K. O.; Geru, I. I.; Dihor, I. N.; Scharff, P.; Eklund, P. C.; Grigorian, L. *Int. J. Thermophys.* **2001**, *22*, 943.
- (17) Adamenko, I. I.; Moroz, K. O.; Prylutsky, Yu. I.; Eklund, P.; Scharff, P.; Braun, T. *Int. J. Thermophys.* **2005**, *26*, 795.
- (18) Scharff, P.; Risch, K.; Carta-Abelmann, L.; Dmytuk, I. M.; Bilyi, M. M.; Golub, O. A.; Khavryuchenko, A. V.; Buzaneva, E. V.; Aksenov, V. L.; Avdeev, M. V.; Prylutsky, Yu. I.; Durov, S. S. *Carbon* **2004**, *42*, 1203.
- (19) (a) Huang, D. M.; Chandler, D. *J. Phys. Chem. B* **2002**, *106*, 2047.  
(b) Chandler, D. *Nature* **2002**, *437*, 491.
- (20) Ashbaugh, H. S.; Paulaitis, M. E. *J. Am. Chem. Soc.* **2001**, *123*, 10721.
- (21) Hernández-Rojas, J.; Bretón, J.; Llorente, J. M. G.; Wales, D. J. *J. Phys. Chem. B* **2006**, *110*, 13357.

- (22) Li, L.; Bedrov, D.; Smith, G. D. *J. Chem. Phys.* **2005**, *123*, 204504.
- (23) Werder, T.; Walther, J. H.; Jaffe, R. L.; Halicioglu, T.; Koumoutsakos, P. *J. Phys. Chem. B* **2003**, *107*, 1345.
- (24) Byl, O.; Liu, J.-C.; Wang, Yim, W.-L.; Johanson, J. K.; Yates, J. T., Jr. *J. Am. Chem. Soc.* **2006**, *128*, 12090.
- (25) Rivelino, R.; Maniero, A. M.; Prudente, F. V.; Costa, L. S. *Carbon* **2006**, *44*, 2925.
- (26) Canuto, S.; Coutinho, K.; Zerner, M. C. *J. Chem. Phys.* **2000**, *112*, 7293.
- (27) (a) Canuto, S.; Coutinho, K.; Trzresniak, D. *Adv. Quantum Chem.* **2002**, *41*, 161. (b) Coutinho, K.; Canuto, S. *J. Chem. Phys.* **2000**, *113*, 9132.
- (28) Georg, H. C.; Coutinho, K.; Canuto, S. *J. Chem. Phys.* **2007**, *126*, 034507.
- (29) Fonseca, T. L.; Coutinho, K.; Canuto, S. *J. Chem. Phys.* **2007**, *126*, 034508.
- (30) Ludwig, V.; Coutinho, K.; Canuto, S. *Phys. Rev. B* **2004**, *70*, 214110.
- (31) (a) Rivelino, R.; Coutinho, K.; Canuto, S. *J. Phys. Chem. B* **2002**, *106*, 12317. (b) Rivelino, R.; Canuto, S.; Coutinho, K. *Braz. J. Phys.* **2004**, *34*, 84.
- (32) Allen, M. P.; Tildesley, D. J. *Computer Simulation of Liquids*; Clarendon Press: Oxford, U.K., 1987.
- (33) Mahoney, M. W.; Jorgensen, W. L. *J. Chem. Phys.* **2000**, *112*, 8910.
- (34) Coutinho, K.; Canuto, S. *DICE: A Monte Carlo Program for Molecular Liquid Simulation*; University of São Paulo: São Paulo, 2000.
- (35) Rivelino, R.; Cabral, B. J. C.; Coutinho, K.; Canuto, S. *Chem. Phys. Lett.* **2005**, *407*, 13.
- (36) (a) Ordejón, P.; Artacho, E.; Soler, J. M. *Phys. Rev. B* **1996**, *53*, 10441. (b) Soler, J. M.; Artacho, E.; Gale, J.; Garcia, A.; Junquera, J.; Ordejón, P.; Sánchez-Portal, D. *J. Phys.: Condens. Matter* **2002**, *14*, 2745.
- (37) Ceperley, D. M.; Alder, B. J. *Phys. Rev. Lett.* **1980**, *45*, 566.
- (38) Perdew, J. P.; Zunger, A. *Phys. Rev. B* **1981**, *23*, 5048.
- (39) (a) Becke, A. D. *Phys. Rev. A* **1998**, *38*, 3098. (b) Lee, C.; Yang, W.; Parr, R. G. *Phys. Rev. B* **1998**, *37*, 785.
- (40) Troullier, N.; Martins, J. L. *Phys. Rev. B* **1991**, *43*, 1993.
- (41) Junquera, J.; Paz, O.; Sánchez-Portal, D.; Artacho, E. *Phys. Rev. B* **2001**, *64*, 235111.
- (42) (a) Artacho, E.; Sánchez-Portal, D.; Ordejón, P.; García, A.; Soler, M. J. *Phys. Status Solidi B* **1999**, *215*, 809. (b) Ordejón, P. *Phys. Status Solidi B* **2000**, *217*, 335.
- (43) Cabral do Couto, P.; Estácio, S. G.; Cabral, B. J. C. *J. Chem. Phys.* **2005**, *123*, 054510.
- (44) Fernandez-Serra, M. V.; Ferlat, G.; Artacho, E. *Mol. Simul.* **2005**, *31*, 361.

NL070308P